

# Dysregulation of T cell receptor N-glycosylation: A molecular mechanism involved in ulcerative colitis

Dias AM<sup>1</sup>, Dourado J, Lago P, Cabral J, Marcos-Pinto R, Salgueiro P, Almeida CR, Carvalho S, Fonseca S, Lima M, Vilanova M, Dinis-Ribeiro M, Reis CA, Pinho SS

1-Institute of Molecular Pathology and Immunology of the University of Porto (IPATIMUP), Porto, Portugal.

This is a pre-copyedited author-produced version of an article accepted for publication in Human Molecular Genetics, following peer review. The version of record Human Molecular Genetics, Volume 23, Issue 9, 1 May 2014, Pages 2416–2427, is available online at: <https://doi.org/10.1093/hmg/ddt632>

## ABSTRACT

The incidence of inflammatory bowel disease is increasing worldwide and the underlying molecular mechanisms are far from being fully elucidated. Herein, we evaluated the role of *N*-glycosylation dysregulation in T cells as a key mechanism in the ulcerative colitis (UC) pathogenesis. The evaluation of the branched *N*-glycosylation levels and profile of intestinal T cell receptor (TCR) were assessed in colonic biopsies from UC patients and healthy controls. Expression alterations of the glycosyltransferase gene *MGAT5* were also evaluated. We demonstrated that UC patients exhibit a dysregulation of TCR branched *N*-glycosylation on lamina propria T lymphocytes. Patients with severe UC showed the most pronounced defect on *N*-glycan branching in T cells. Moreover, UC patients showed a significant reduction of *MGAT5* gene transcription in T lymphocytes. In this study, we disclose for the first time that a deficiency in branched *N*-glycosylation on TCR due to a reduced *MGAT5* gene expression is a new molecular mechanism underlying UC pathogenesis, being a potential novel biomarker with promising clinical and therapeutic applications.

## INTRODUCTION

Inflammatory bowel disease (IBD) is a chronic immune-mediated disorder of the gastrointestinal tract that includes ulcerative colitis (UC) and Crohn's disease (CD) (1). The incidence of IBD is

INSTITUTO  
DE INVESTIGAÇÃO  
E INOVAÇÃO  
EM SAÚDE  
UNIVERSIDADE  
DO PORTO

increasing worldwide and the disease remains incurable. IBD places a heavy burden on populations reducing quality of life and incurring substantial medical and societal costs (2). Although progress has been made in understanding the disease, the etiopathogenesis of IBD is far from being fully elucidated. Accumulating evidence suggests that IBD results from an inappropriate inflammatory response in a genetically susceptible host (1,3), although the underlying molecular mechanisms remain elusive.

UC is a chronic inflammatory condition causing continuous mucosal inflammation of the colon affecting the rectum and a variable extent of the colon in continuity, which is characterized by a relapsing and remitting course. The inflammation in UC is typically confined to the mucosa (1,2), and the course of the disease is characterized by flares that alternate with periods of remission. Severity of flares and their response to treatment vary and are hard to predict. In addition, prognosis of patients with UC is difficult to determine (2). In line with this, it is of paramount importance to further identify and characterize the underlying molecular mechanisms of UC pathogenesis in order to improve the development of novel biomarkers that may help the determination of prognosis and also improve the patients' stratification for appropriate treatment (4).

Glycosylation is a complex post-translational mechanism characterized by the addition of carbohydrate structures (glycans) to proteins and lipids in the endoplasmic reticulum/Golgi secretory pathway, by specific enzymes (glycosyltransferases) (5). The immune system is tightly controlled by cellular glycosylation as almost all of the key molecules involved in innate and adaptive immune responses are glycoproteins (6–8). The *N*-acetylglucosaminyltransferase V (GnT-V) is a glycosyltransferase encoded by the human *MGAT5* gene that catalyses the synthesis of  $\beta$ 1,6 GlcNAc branched *N*-glycans structures, which are known to play pivotal roles in many glycoproteins in cancer (9,10), and particularly in T cell function (11). This *N*-glycan branch commonly includes polylactosamine chains (*N*-acetylglucosamine disaccharide repeats) that are ligands for various lectins of the galectin family (12). Mice deficient in the *MGAT5* gene have been shown to develop autoimmune diseases, increased delayed-type hypersensitivity responses and an enhanced susceptibility to experimental autoimmune encephalomyelitis (EAE, a mouse model of multiple sclerosis) (13–15). These mice lacking GnT-V function (no synthesis of  $\beta$ 1,6GlcNAc branched *N*-glycans structures) display a significantly increased T cell receptor (TCR) clustering, leading to a decreased threshold of T cell activation, and increased  $T_H1$  differentiation resulting in hyperimmune response and increased susceptibility to autoimmunity (16,17). Overall, these reports support that T cell activity and signaling is tightly regulated by GnT-V-mediated glycosylation. In fact, in homeostasis and self-tolerance, T cell activation (TCR signaling) induces up-regulation of *MGAT5* gene which in turns leads to GnT-V-mediated glycosylation of the TCR (18). This phenotype promotes growth arrest of T cells by at least two mechanisms: early, by raising T cell activation thresholds via limiting TCR clustering at the immune synapse and the consequent hyperimmune response, and later by increasing surface retention of growth inhibitory receptors such as cytotoxic T lymphocyte antigen-4 (CTLA-4) (18).

The abovementioned evidences in other immune-mediated disorders set the ground to the present study that aims to address for the first time whether the dysregulation of this critical interplay between *N*-glycan branching and T cell activity is a major contributory factor and a yet uncovered mechanism underlying UC. In this study, we first report that dysregulation of the GnT-V-mediated glycosylation of the TCR on lamina propria T cells is a new molecular mechanism underlying UC

pathogenesis. We further showed that UC patients exhibit a deficiency in T lymphocytes *MGAT5* gene transcription comparing with normal controls, which underlies the observed dysregulation of T cell glycosylation in UC.

## RESULTS

### Active UC cases exhibit a decreased expression of branched *N*-glycans in intestinal lymphocytic infiltrates

We first evaluated whether there were alterations in the expression of  $\beta_{1,6}$  GlcNAc branched *N*-glycans structures in intestinal lamina propria lymphocytic infiltrates positive for CD3 expression in a well-characterized series of colonic biopsies ( $n = 64$ ) from UC patients comparing with normal controls. By using L-PHA lectin histochemistry, we observed that active UC cases had significantly lower expression ( $P < 0.0001$ ) of branched *N*-glycans in intestinal lamina propria cell infiltrates CD3<sup>+</sup>, when compared with normal controls (Table 1, Fig. 1A and B). UC patients with inactive disease (Mayo subscore 0), which have a controlled T cell response, showed increased expression of lymphocytic branched *N*-glycans expression (Table 1) comparing with active UC (Mayo subscore  $\geq 1$ ), but a tendency to have less lymphocytic *N*-glycans expression levels than normal controls. In the controls, the lamina propria lymphocytes (LPLs) CD3<sup>+</sup> exhibit high expression of L-PHA lectin (Table 1, Fig. 1A and B). No differences were observed comparing the levels of L-PHA expression with age, gender and disease extension. These results showed significant alterations of  $\beta_{1,6}$  GlcNAc branched *N*-glycans expression in the intestinal lymphocytic infiltrate of UC cases comparing with normal controls. The variability in branched *N*-glycans expression on T cells among active and inactive UC is in accordance with disease severity. All of the severe UC cases (Mayo subscore 3) showed the lowest expression (<25%) of lymphocytic branched *N*-glycans. Moreover, we have observed that, for the same patient and during the course of disease, the percentage of expression of lymphocytic branched *N*-glycans varies accordingly with disease severity. These results were next explored in-depth at the molecular level.

### Levels of TCR and CD3 expression in UC patients and normal controls: phenotypic characterization of T cells subsets and activation state

The results showed increasing levels of TCR $\beta$  and CD3 protein expression from normal controls; inactive UC (Mayo subscore 0); to active UC patients (Mayo subscore  $\geq 1$ ). The severe UC patients (Mayo subscore 3) had the higher levels of both TCR $\beta$  and CD3 proteins of the analyzed samples groups (Fig. 2A). The TCR $\beta$  and CD3 protein expression levels correlated with the clinical criterions; Mayo endoscopic subscore and the histological standards for these setting of patients. In addition, the isolated T cells obtained from the fresh colonic biopsies were analyzed by imaging flow cytometry analysis (Fig. 2C). The results showed that the expression of TCR from isolated cells were higher in active UC patients comparing with normal controls (Fig. 2C), validating the results obtained by western blot (Fig. 2A and B).

The phenotypic characterization of the T cells subsets showed that the intestinal T cell lymphocytic infiltrate from UC patients is predominantly represented by CD4<sup>+</sup> T cells, whereas in the normal individuals the intestinal T cells population is predominantly CD8<sup>+</sup> (Fig. 2D and E). Curiously, intestinal T cells from patients with UC had higher levels of TCR-alpha/beta expression when compared with intestinal T cells from controls (Fig. 2C and D), this being more evident in CD4<sup>+</sup> T cells than in CD8<sup>+</sup> T cells (data not shown). In addition, both normal and UC intestinal T cells express activation-related markers, HLA-DR and CD45RO (Fig. 2D and E). However, intestinal T cells from UC patients exhibit a higher level of expression of these activation-related markers compared with controls, as evaluated by the median fluorescence intensity (MFI) of the antigen expression (Fig. 2E).

### TCRs from UC patients exhibit a decreased modification with $\beta$ 1,6 GlcNAc branched N-glycans structures

In order to evaluate the levels of  $\beta$ 1,6 GlcNAc branched N-glycans expression specifically on the TCR of LPLs from UC patients and controls, we performed different experimental approaches that mutually validate each other. On the one hand, we isolated the LPLs from a subset of fresh biopsies collected from UC patients and controls which were analyzed by the L-PHA blot. We demonstrated that the TCR was differently glycosylated with branched N-glycans compared with UC patients and normal controls (Fig. 3A and B). UC patients with active disease (Mayo subscore  $\geq 1$ ) showed a significant decrease in the levels of TCR modification with branched N-glycans when compared with controls. Patients with severe disease (Mayo subscore 3) displayed the lowest levels of TCR glycosylation. Moreover, the levels of branched N-glycans modification on the TCR surface decreased concomitantly with disease severity (from Mayo subscore 0 to 3) (Fig. 3A and B), as also observed by histochemistry (Table 1 and Fig. 1). The levels of bisecting GlcNAc structures (catalyzed by GnT-III) on the TCR did not vary significantly among UC patients and controls (Supplementary Material, Fig. S1). These results on the isolated LPLs were further validated, by performing TCR immunoprecipitation from the total protein lysate (TCL) of the UC and controls biopsies, followed by  $\beta$ 1,6 GlcNAc branched N-glycans recognition (L-PHA blot) (Fig. 3C and D). The results demonstrated that UC patients (both with inactive and active disease) showed significant decreased levels of TCR glycosylation with branched N-glycan structures compared with normal controls. Again, patients with severe disease (Mayo subscore 3) showed the lowest levels of  $\beta$ 1,6 GlcNAc branched N-glycans on TCR. These observations obtained at the molecular level by two different technical approaches, pinpoint the existence of a dysregulation of intestinal TCR N-glycosylation mediated by GnT-V in UC patients compared with controls, which appear to be associated with disease severity. Furthermore, we also confirm this dysregulation by imaging flow cytometry that combines features of both conventional flow cytometry and fluorescence microscopy and thus allows quantification of imaging parameters, including membrane intensity of different probes (19). Interestingly, we observed that isolated LPLs from active UC patients showed a decreased fluorescence intensity of L-PHA on the membrane of the TCR $\alpha/\beta$  positive cells than the one detected in normal controls (Fig. 4). These bioimaging observations corroborate the above results and further pointing toward a deficiency in TCR branched N-glycans in UC patients.

## MGAT5 gene expression alterations in T cells from UC patients

It has been demonstrated that TCR signaling regulates multiple Golgi *N*-glycan branching-processing enzymes at the mRNA level, such as *MGAT5* (18). Therefore, and in order to assess if the deficiency in TCR *N*-glycan branching, catalyzed by GnT-V, could be due to genetic alterations of *MGAT5* glycogene, we evaluated the mRNA transcription levels of *MGAT5* in a representative sub-series of intestinal LPLs isolated from active UC patients and normal controls (Fig. 5A and B). Our results consistently showed that LPLs from UC patients with active disease significantly express altered mRNA levels of *MGAT5* compared with normal controls (Fig. 5). The *MGAT5* mRNA analysis performed both independently (Fig. 5A) or using RNA pooled from different individuals (Fig. 5B) showed that LPLs from active UC patients had significantly lower levels of *MGAT5* transcription than normal controls. No significant alterations were observed on *MGAT3* transcription ([Supplementary Material, Fig. S1](#)). This is the first evidence suggesting the identification of a possible genetic alteration in the *MGAT5* gene from LPLs, which appears to underlie the deficiency of TCR *N*-glycosylation associated with UC pathogenesis, an issue that is being further studied in larger cohort populations.

## DISCUSSION

In the present study, we have disclosed a novel molecular mechanism contributing for UC pathogenesis. We demonstrated that UC patients have dysregulation of intestinal TCR *N*-glycosylation, which has been associated with T cell hyperactivity and hyperimmune response (16,17). We further provide the first evidence supporting that UC patients exhibit a transcriptional alteration of the *MGAT5* gene in intestinal LPLs that appear to be the causative mechanism for the deficiency on TCR *N*-glycosylation of these patients, which associates with, and may possibly determine disease severity or susceptibility.

A growing body of evidence has demonstrated that in homeostasis and self tolerance, the T cell activation (TCR signaling) induces up-regulation of the *MGAT5* gene which in turns leads to GnT-V-mediated glycosylation of the TCR (18). The *N*-glycan branching on T cells, catalyzed by GnT-V glycosyltransferase, promotes the formation of multivalent galectin binding which negatively regulates T cell growth by precluding TCR clustering, and increasing the TCR activation thresholds, ultimately modulating the immune response (Fig. 6). Interestingly, recent evidences support that environmental and genetic dysregulation of *N*-glycosylation are involved in the molecular mechanism of human multiple sclerosis pathogenesis (15,20). In UC we consistently observed, both by immunohistochemistry and at molecular level, that UC patients exhibit a defective *N*-glycan branching on intestinal TCR compared with normal controls (Fig. 6). Interestingly, patients with severe forms of endoscopic activity (Mayo endoscopic subscore 3) showed the lowest levels of TCR *N*-glycan branching compared with patients with mild, moderate or inactive disease. This variability in the levels of TCR *N*-glycan branching among UC patients was demonstrated to accompany disease severity, which at the end may determine different susceptibilities to the different forms of UC. These data are in accordance with previous observations in models of EAE (21). The authors reported that among inbred mouse strains, *N*-glycan GlcNAc branching in T cells

was highly variable (different hypomorphic forms) and inversely correlated with EAE susceptibility (21). In addition, we observed that levels of TCR glycosylation are associated with different T cell subsets (predominantly represented by CD4<sup>+</sup> T cells in UC patients and by CD8<sup>+</sup> T cells in normal individuals) and with different levels of T cell activation (higher surface expression of HLA-DR and CD45RO on T cells from UC patients, when compared with controls). Lower levels of TCR glycosylation (in UC patients) were found in the intestinal T cell subsets that were predominantly represented by CD4<sup>+</sup> T cells in an activated state. These differences on TCR branched glycosylation associated with different T cells subsets/activation (Fig. 2D and E) are in accordance with previous observations showing that CD4<sup>+</sup> and CD8<sup>+</sup> T cells have been shown to have different profiles of *N*-linked glycans (22,23). Differential effects of glycosylation on specific T cell lineages have been reported previously. For instance, sialyltransferase ST3 Gal-I-deficient mice lacked CD8<sup>+</sup>, but not CD4<sup>+</sup> T lymphocytes (24). Moreover, and in line with our observations, the disruption of *N*-glycosylation by *MGAT5* ablation has been shown to lower T lymphocyte activation thresholds and cause autoimmunity (17). Altogether, our results further support that the differential glycosylation of CD4<sup>+</sup> versus CD8<sup>+</sup> T cells could cause differential activation thresholds and/or mechanisms (23). In addition, these glycosylation differences in the T cells subsets compared UC patients and controls may have major impact on CD4<sup>+</sup> versus CD8<sup>+</sup> T cell differentiation and function. This issue should be further examined in the future. To further explore the possible causative mechanism of the dysregulation of the TCR branched *N*-glycosylation in UC patients, we evaluated the mRNA transcription levels of the *MGAT5* gene (that encodes GnT-V enzyme). Interestingly, we consistently observed a reduced *MGAT5* mRNA transcription levels in LPLs from UC patients with active disease compared with controls. These results support a genetic alteration of the *MGAT5* gene from intestinal T lymphocytes of UC patients, being the underlying event that promotes a dysregulated immune response through a disturbance in protein branched *N*-glycosylation catalyzed by GnT-V on intestinal TCR (Fig. 6). Interestingly, and in line with our results, it has been proposed that *MGAT5* is a gene that determines severity and susceptibility to multiple sclerosis (25,26). Our observations open new avenues for further exploring *MGAT5* as a potential susceptibility gene in IBD pathogenesis. Nevertheless, whether this dysregulation of *MGAT5*/GnT-V-mediated glycosylation on TCR is a cause or consequence of the Ulcerative Colitis disease is a premature conclusion that deserves to be carefully addressed.

In addition, the identification of a specific molecular mechanism underlying UC pathogenesis constitutes an opportunity to improve the target-specific therapy of UC patients. In fact, it was showed that metabolic supplementation of mice or T cells with UDP-GlcNAc enhances GlcNAc branching of T cells catalyzed by GnT-V which increases the threshold for T cell activation, suppresses T cell growth and inhibits Th1 differentiation leading to a controlled immune response and a decreased disease clinical severity in EAE and type I non-obese diabetic mice (27,28). Interestingly enough, a pilot study of oral GlcNAc in pediatric treatment-resistant IBD reveals the potential of GlcNAc as a therapeutic agent. In that pilot study, 8 out of 12 children with severe IBD went into clinical remission with evidence of histological improvement (29). Our results further contribute to explain the therapeutic effect of GlcNAc observed in pediatric IBD that was at that time unknown. The identification of an underlying disease mechanism prone to be targeted by specific therapy is a major unmet need for the management of IBD in general, enlarging the therapeutic options and improving the success of the therapy. In this regard, we are conducting further studies and controlled trials in order to test the therapeutic efficacy of this inexpensive and non-toxic agent in IBD.

In conclusion, our study demonstrates that dysregulation of branched *N*-glycosylation on TCR is a key mechanism in UC pathogenesis. Moreover, we identified that *MGAT5* gene expression alterations underlie the observed defect on TCR branched *N*-glycosylation. This deficiency in T cells *N*-glycosylation is positively associated with disease severity. Taken together, the disclosure of this new molecular mechanism in UC disease opens new windows of opportunity to further explore the potential applicability of this mechanism in predicting disease course and/or susceptibility. In addition, our observations further suggest the potential of metabolic supplementation with GlcNAc as a promising therapeutic tool that directly targets an underlying mechanism.

## MATERIALS AND METHODS

### Patient selection and colonic biopsies collection

The present study includes 30 patients from which 13 were normal controls and 17 were IBD patients diagnosed with UC that underwent scheduled colonoscopy (between 1991 and 2013) at the Gastroenterology Department of Centro Hospitalar do Porto-Hospital de Santo António (CHP/HSA), Porto, Portugal. The patients were randomly enrolled in the study prospectively from a cohort of outpatients of IBD clinics. All the 17 patients were studied: retrospectively by analyzing formalin-fixed paraffin-embedded (FFPE) samples at different stages of disease course/activity (obtained from the Pathology archive of CHP/HSA); and prospectively, where collected fresh colonic biopsies (8–20 biopsies per UC patient) were analyzed for different purposes: histology/morphology; isolation LPLs; protein and RNA extraction. From these 17 UC patients, we have analyzed 51 colonic biopsies (FFPE samples) that were collected at different times of the disease course. The fresh biopsies ( $n = 8–20$  per UC patient) were representative of macroscopically active/inactive disease topography, as defined by Mayo endoscopic score (UC samples). Eligibility criteria for inclusion in this study were no history of human immunodeficiency virus. Age and gender were not exclusion factors (Table 2). Patients with UC were excluded if they had evidence of dysplasia or malignancy on colonoscopy with biopsy or positive to *Clostridium difficile* or infectious agents in stool assay in active UC cases. Cytomegalovirus (CMV) infection was also excluded using histopathology combined with immunohistochemistry against CMV antigens. Endoscopic assessment of the severity of UC was determined using the Mayo endoscopic subscore for UC as follows: normal or inactive disease—subscore 0; mild disease—subscore 1 (erythema, decreased vascular pattern, mild friability); moderate disease—subscore 2 (marked erythema, lack of vascular patterns, friability, erosions); severe disease—subscore 3 (spontaneous bleeding, ulceration) (30,31).

Normal controls ( $n = 13$ ) were randomly enrolled in the study (prospectively) and were represented by individuals that attend the gastroenterology department of CHP-HSA for a planned colonoscopy. The control group includes individuals without detectable colorectal lesions or previous history of IBD, colorectal hereditary syndromes or cancer (adenocarcinomas). In the patients of the control group, biopsies (8–20 biopsies per control used for the different purposes) were performed in mucosa without endoscopic abnormalities.

All specimens were subjected to histological examination and classification. All participants gave informed consent about all clinical procedures and research protocols were approved by the ethics committee of CHP/HSA, Portugal (233/12(179-DEFI/177-CES).

Overall, we have analyzed 64 FFPE colonic biopsy samples. In addition, from a subset of UC patients and controls, we have also analyzed fresh colonic biopsies at different stages of disease course which were collected prospectively from 2011 to 2013.

### Tissue histochemistry

A total of 64 FFPE colonic biopsies from normal controls (n = 13) and UC patients (n = 51) (16 Mayo subscore 0; 13 Mayo subscore 1; 14 Mayo subscore 2; 8 Mayo subscore 3) were analyzed by histochemistry in order to evaluate the expression of CD3 and the  $\beta$ 1,6GlcNAc branched N-glycan structures.

Identification of intestinal T lymphocytes at lamina propria was performed by CD3 immunohistochemistry. Heat-induced antigen retrieval was performed and endogenous peroxidase activity was blocked. Slides were washed and incubated with swine normal serum (Dako) before incubation with rabbit IgG anti-human CD3 monoclonal antibody (clone EP449E, Thermo Scientific, diluted at 1:50) overnight, at 4°C. The slides were washed and incubated with biotinylated swine anti-rabbit secondary antibody (Dako).

For evaluation of the expression of  $\beta$ 1,6 GlcNAc branched structures, sections were incubated 1 h with biotinylated Phaseolus Vulgaris Leucoagglutinin (L-PHA) lectin that specifically recognizes the  $\beta$ 1,6GlcNAc branched N-glycan structures (Vector Laboratories) diluted at 1:150.

The avidin–biotin–peroxidase complex detection method was the Vectastain ABC Kit (Vector Laboratories). The chromogen used was 3,30-diaminobenzidine (DAB). Sections were counterstained with hematoxylin, dehydrated and mounted. Controls were incubated with PBS instead of the primary antibody or lectin. As positive control, sections of thymus (for CD3 expression) and colon carcinoma (for L-PHA staining) were used. The percentage of expression of the  $\beta$ 1,6 GlcNAc branched structures (L-PHA reactivity) in the intestinal lymphocytic infiltrate (T cells at lamina propria) positive to CD3 were evaluated by three independent observers (J.C.; S.S.P.; C.A.R.) and scored as follows: less than 25%; 25–50%; 50–75% and more than 75% of intestinal T lymphocytes at lamina propria stained. For statistical analysis, the percentage of expression of L-PHA lectin reactivity was regrouped into two percentual categories ( $\leq$ 25%: low expression; and  $>$ 25% to  $\geq$ 75%: high expression) in order to increase the number of cases in each category and in this manner improve the statistical power of the tests.

The statistical relationship among variables was analyzed in StatView (SAS Institute) using tables of frequencies and their significance tested by the Chi-square ( $\chi^2$ ). P-values less than 0.05 were considered a significant association.

### Isolation of LPLs

LPLs were isolated from fresh colonic biopsies, following an adapted protocol (32). In order to isolate the LPLs, Percoll (Sigma) density gradients were used (1.05–1.09 g/ml). Lymphocytes were washed twice and cell yields were determined using a hemacytometer and cell viability was determined by trypan blue exclusion. After LPLs isolation, the levels of CD3 and/or TCR expression were evaluated by flow cytometry and/or imaging flow cytometry analysis.

### Flow cytometry

To perform the characterization of the T cells subsets and activation state, isolated LPLs from normal individuals (n = 2 biological replicates) and UC patients (n = 2 biological replicates) were resuspended in 1000  $\mu$ l of FACS Buffer (PBS1x containing 0.1% sodium azide and 2% BSA) following 15 min of incubation at room temperature with the appropriate volume of monoclonal antibodies specific for CD45 (clone G490, IgG2a mouse; Cytognos SL, Salamanca, Spain), CD3 (clone SK7, IgG1 mouse; Becton Dickinson Biosciences, California, USA—BDB), TCR-alpha/beta (clone T10B9.1A-31, IgM mouse; BD Pharmingen, California, USA), CD4 (clone SK3, IgG2a mouse; BDB), CD8 (clone SK1, IgG1 mouse; BDB), CD45RO (clone UCHL-1BDB, IgG2a mouse; BDB) and HLA-DR (clone Immu-357, IgG1 mouse; Immunotech, Marseille, France—IOT), conjugated with orange cytognos 550 (OC550), pacific blue (PB), fluorescein isothiocyanate (FITC), peridinin-chlorophyll-protein complex Cy5.5 tandem (PerCP-Cy5.5), allophycocyanin (APC), phycoerythrin (PE) and phycoerythrin-Cy7 tandem (PE-Cy7), respectively. Lastly, cells were fixed with 4% formaldehyde. Data acquisition was performed in a FACS Canto v.2 flow cytometer (BDB), using the FACSDiva software (BDB). Instrument alignment and standardization were done according to the recommendations of the Euroflow consortium. Data on a minimum of  $2 \times 10^5$  events were acquired for each staining. The data were analyzed using the Infinicyt™ software (Cytognos SL). Lymphocytes were first identified and gated based on their bright CD45 expression and light scatter characteristics, and T cells were gated based on the expression of surface CD3. Afterwards, the major T-cell populations were identified and quantified, based on the type of TCR receptor (alpha/beta and gamma-delta), and CD4/CD8 molecules (CD4+, CD8+ and CD4–CD8– T cells). Finally, T cells were characterized for the expression of the activation-related markers, CD45RO and HLA-DR. Results were expressed as percentage (%) of cells that stained positively for each analyzed antigen, as well as the MFI due to antigen staining.

## Imaging flow cytometry

Isolated LPLs were centrifuged and the pellets resuspended in FACS Buffer. For TCR staining, cells were incubated with anti-TCR $\alpha/\beta$  mAb (clone BW242/412 mouse IgG2b) conjugated with R-phycoerythrin (PE) (Miltenyi Biotec) diluted in FACS Buffer, on ice for 30 min, in the dark. For L-PHA staining, cells were then incubated with L-PHA/FITC (4  $\mu$ g/ml) (Vector Laboratories) and as negative control cells were incubated with Streptavidin-conjugated fluorescein isothiocyanate (FITC) (1  $\mu$ g/ml) (Caltag Laboratories). Afterwards cells were washed, fixed with 4% formaldehyde and analyzed by imaging flow cytometry.

Images of isolated cells were acquired on a 6-Channel ImageStreamX Imaging Flow Cytometer (Amnis, EMD Millipore) at the Bioimaging Center for Biomaterials and Regenerative Therapies (b.IMAGE, INEB, Porto, Portugal). Analysis was performed with IDEAS 5.0 (Amnis, EMD Millipore). Upon compensation, co-localization of the TCR $\alpha/\beta$  protein with L-PHA was determined with co-localization wizard. The intensity of L-PHA staining within the TCR $\alpha/\beta$  positive events was also determined. The experiment was reproduced two times using cells from two different biological replicas.

## Western-blot and immunoprecipitation

Evaluation of the total protein expression levels of TCR and CD3 was performed using 40  $\mu$ g of TCL obtained from the whole fresh biopsy digestion. The samples were subjected to 12% SDS-PAGE electrophoresis and membranes were blocked before incubation with primary antibodies against TCR $\beta$  (mouse monoclonal antibody anti-human, Santa Cruz Biotechnology) (dilution 1:100) and CD3 (rat anti-human CD3 $\epsilon$  mAb, Cell Signaling Technologies) (dilution 1:1000). The respective secondary antibodies used were goat anti-mouse IgG-HRP (Santa Cruz Biotechnology) and donkey anti-rat IgG-HRP (Jackson ImmunoResearch). For loading control analysis, mouse IgG anti-tubulin (Sigma) was used. The target proteins were visualized using ECL reagent (GE Healthcare, Life Sciences).

For TCR immunoprecipitation (IP), equal amounts of TCL obtained from the whole biopsy (500  $\mu$ g) were precleared with protein G-sepharose beads (GE Healthcare, Life Sciences) and the supernatant was incubated overnight with rabbit anti-human TCR $\beta$  polyclonal antibody (Santa Cruz Biotechnology). The immune complexes were released by boiling and subjected to 12% SDS-PAGE. Membranes were blocked and probed with the primary anti-human TCR $\beta$  polyclonal antibody (dilution 1:100), and revealed with secondary antibody goat anti-rabbit IgG-HRP (Santa Cruz Biotechnology). For the  $\beta$ 1,6 GlcNAc branched structures analysis on TCR, membranes were probed with biotinylated L-PHA or E-PHA (10  $\mu$ g/ml) lectin. Immunoreactive bands were then visualized using the Vectorstain ABC kit and detection was performed by an ECL reagent. Quantitative analyses were performed by densitometric scanning of bands.

For L-PHA or E-PHA lectin blot analysis, 20 µg of LPLs protein lysate was used. Membranes were blocked before incubation with L-PHA or E-PHA lectin and bands were then visualized using the Vectorstain ABC kit. The detection was performed by an ECL reagent. For loading control, anti-tubulin mAb was used.

The experiments were reproduced at least three times. For all data comparisons, the Student's t-test was used (two tailed, unequal variance). Results were considered statistically significant when  $P < 0.05$ .

### Real-time PCR

Total RNA from isolated LPLs was extracted with Tri-Reagent (Sigma) or RNAqueous- Micro Kit (Applied Biosystems) according to the manufacturer's protocol. The quantitative real-time PCR (qRT-PCR) was performed using TaqMan Gene Expression Assays (Applied Biosystems). T lymphocytes total RNA were reversed transcribed to single-stranded cDNA using random hexamer primers and Superscript II Reverse Transcriptase (Invitrogen). qRT-PCR was carried out in triplicates using RNA source from three biological replicates (three normal individuals and three UC patients) and RNA pooled from four different normal controls and four different UC patients with active disease, for the target genes MGAT5 (Taqman probe: hs.00159136\_m1, Applied Biosystems), MGAT3 (Taqman probe: hs.02379589\_s1, using RNA source from 2 biological replicates: two normal individuals and two UC patients) and for the appropriated lymphocytes endogenous control 18S (Hs.PT.39a.22214856.g, Integrated DNA Technologies) and qRT-PCR reactions were performed on the ABI Prism 7000 Sequence Detection System. Data were analyzed by the comparative  $2(-\Delta\Delta CT)$  method (33). For all data comparisons, the Student's t-test was used (two-tailed, unequal variance). Results were considered statistically significant when  $P < 0.05$ .

### SUPPLEMENTARY MATERIAL

Supplementary Material is available at HMG online.

*Conflict of Interest statement.* None declared.

## FUNDING

This work was supported by grants from the Portuguese Foundation for Science and Technology (FCT), project grants (PTDC/CVT/111358/2009; PTDC/BBB-EBI/0786/2012; EXPL/BIM-MEC/0149/2012), 'financiados no âmbito do Programa Operacional Temático Factores de Competitividade (COMPETE) e participado pelo fundo Comunitário Europeu FEDER', e do Quadro de Referência Estratégia Nacional QREN. This work was further supported by a portuguese grant from 'Grupo de Estudo da Doença Inflamatória Intestinal' (GEDII). S.S.P. (SFRH/BPD/63094/2009); S.C. (SFRH/BD/77386/2011) also acknowledge FCT. IPATIMUP is an Associate Laboratory of the Portuguese Ministry of Science, Technology and Higher Education, and is partially supported by FCT.

**INSTITUTO  
DE INVESTIGAÇÃO  
E INOVAÇÃO  
EM SAÚDE**  
UNIVERSIDADE  
DO PORTO

## REFERENCES

1. Abraham, C. and Cho, J.H. (2009) Inflammatory bowel disease. *N. Engl. J. Med.*, 361, 2066–2078.
2. Cosnes, J., Gower-Rousseau, C., Seksik, P. and Cortot, A. (2011) Epidemiology and natural history of inflammatory bowel diseases. *Gastroenterology*, 140, 1785–1794.
3. Xavier, R.J. and Podolsky, D.K. (2007) Unravelling the pathogenesis of inflammatory bowel disease. *Nature*, 448, 427–434.
4. Plevy, S.E. and Targan, S.R. (2011) Future therapeutic approaches for inflammatory bowel diseases. *Gastroenterology*, 140, 1838–1846.
5. Ohtsubo, K. and Marth, J.D. (2006) Glycosylation in cellular mechanisms of health and disease. *Cell*, 126, 855–867.
6. Marth, J.D. and Grewal, P.K. (2008) Mammalian glycosylation in immunity. *Nat. Rev. Immunol.*, 8, 874–887.
7. Rudd, P.M., Elliott, T., Cresswell, P., Wilson, I.A. and Dwek, R.A. (2001) Glycosylation and the immune system. *Science*, 291, 2370–2376.
8. Rabinovich, G.A., van Kooyk, Y. and Cobb, B.A. (2012) Glycobiology of immune responses. *Ann. N. Y. Acad. Sci.*, 1253, 1–15.
9. Pinho, S.S., Figueiredo, J., Cabral, J., Carvalho, S., Dourado, J., Magalhaes, A., Gartner, F., Mendonça, A.M., Isaji, T., Gu, J. et al. (2013) E-cadherin and adherens-junctions stability in gastric carcinoma: functional implications of glycosyltransferases involving N-glycan branching biosynthesis, N-acetylglucosaminyltransferases III and V. *Biochim. Biophys. Acta*, 1830, 2690–2700.
10. Pinho, S.S., Reis, C.A., Paredes, J., Magalhaes, A.M., Ferreira, A.C., Figueiredo, J., Xiaogang, W., Carneiro, F., Gartner, F. and Seruca, R. (2009) The role of N-acetylglucosaminyltransferase III and V in the post-transcriptional modifications of E-cadherin. *Hum. Mol. Genet.*, 18, 2599–2608.
11. Daniels, M.A., Hogquist, K.A. and Jameson, S.C. (2002) Sweet 'n' sour: the impact of differential glycosylation on T cell responses. *Nat. Immunol.*, 3, 903–910.
12. Garner, O.B. and Baum, L.G. (2008) Galectin-glycan lattices regulate cell-surface glycoprotein organization and signalling. *Biochem. Soc. Trans.*, 36, 1472–1477.
13. Granovsky, M., Fata, J., Pawling, J., Muller, W.J., Khokha, R. and Dennis, J.W. (2000) Suppression of tumor growth and metastasis in Mgat5-deficient mice. *Nat. Med.*, 6, 306–312.
14. Grigorian, A. and Demetriou, M. (2011) Mgat5 deficiency in T cells and experimental autoimmune encephalomyelitis. *ISRN Neurol.*, 2011, 374314.

15. Mkhikian, H., Grigorian, A., Li, C.F., Chen, H.L., Newton, B., Zhou, R.W., Beeton, C., Torossian, S., Tatarian, G.G., Lee, S.U. et al.. (2011) Genetics and the environment converge to dysregulate N-glycosylation in multiple sclerosis. *Nat. Commun.*, 2, 334.
16. Morgan, R., Gao, G., Pawling, J., Dennis, J.W., Demetriou, M. and Li, B. (2004) N-acetylglucosaminyltransferase V (Mgat5)-mediated N-glycosylation negatively regulates Th1 cytokine production by T cells. *J. Immunol.*, 173, 7200–7208.
17. Demetriou, M., Granovsky, M., Quaggin, S. and Dennis, J.W. (2001) Negative regulation of T-cell activation and autoimmunity by Mgat5 N-glycosylation. *Nature*, 409, 733–739.
18. Chen, H.L., Li, C.F., Grigorian, A., Tian, W. and Demetriou, M. (2009) T cell receptor signaling co-regulates multiple Golgi genes to enhance N-glycan branching. *J. Biol. Chem.*, 284, 32454–32461.
19. Basiji, D.A., Ortyn, W.E., Liang, L., Venkatachalam, V. and Morrissey, P. (2007) Cellular image analysis and imaging by flow cytometry. *Clin. Lab. Med.*, 27, 653–670, viii.
20. Grigorian, A., Mkhikian, H., Li, C.F., Newton, B.L., Zhou, R.W. and Demetriou, M. (2012) Pathogenesis of multiple sclerosis via environmental and genetic dysregulation of N-glycosylation. *Semin. Immunopathol.*, 34, 415–424.
21. Lee, S.U., Grigorian, A., Pawling, J., Chen, I.J., Gao, G., Mozaffar, T., McKerlie, C. and Demetriou, M. (2007) N-glycan processing deficiency promotes spontaneous inflammatory demyelination and neurodegeneration. *J. Biol. Chem.*, 282, 33725–33734.
22. Comelli, E.M., Sutton-Smith, M., Yan, Q., Amado, M., Panico, M., Gilmartin, T., Whisenant, T., Lanigan, C.M., Head, S.R., Goldberg, D. et al. (2006) Activation of murine CD4<sup>+</sup> and CD8<sup>+</sup> T lymphocytes leads to dramatic remodeling of N-linked glycans. *J. Immunol.*, 177, 2431–2440.
23. Rossi, N.E., Reine, J., Pineda-Lezamis, M., Pulgar, M., Meza, N.W., Swamy, M., Risueno, R., Schamel, W.W., Bonay, P., Fernandez-Malave, E. et al. (2008) Differential antibody binding to the surface alpha beta TCR.CD3 complex of CD4<sup>+</sup> and CD8<sup>+</sup> T lymphocytes is conserved in mammals and associated with differential glycosylation. *Int. Immunol.*, 20, 1247–1258.
24. Priatel, J.J., Chui, D., Hiraoka, N., Simmons, C.J., Richardson, K.B., Page, D.M., Fukuda, M., Varki, N.M. and Marth, J.D. (2000) The ST3Gal-I sialyltransferase controls CD8<sup>+</sup> T lymphocyte homeostasis by modulating O-glycan biosynthesis. *Immunity*, 12, 273–283.
25. Brynedal, B., Wojcik, J., Esposito, F., Debailleul, V., Yaouanq, J., Martinelli-Boneschi, F., Edan, G., Comi, G., Hillert, J. and Abderrahim, H. (2010) MGAT5 alters the severity of multiple sclerosis. *J. Neuroimmunol.*, 220, 120–124.
26. Li, C.F., Zhou, R.W., Mkhikian, H., Newton, B.L., Yu, Z. and Demetriou, M. (2013) Hypomorphic MGAT5 polymorphisms promote multiple sclerosis cooperatively with MGAT1 and interleukin-2 and 7 receptor variants. *J. Neuroimmunol.*, 256, 71–76.

27. Grigorian, A., Lee, S.U., Tian, W., Chen, I.J., Gao, G., Mendelsohn, R., Dennis, J.W. and Demetriou, M. (2007) Control of T Cell-mediated autoimmunity by metabolite flux to N-glycan biosynthesis. *J. Biol. Chem.*, 282, 20027–20035.
28. Grigorian, A., Araujo, L., Naidu, N.N., Place, D.J., Choudhury, B. and Demetriou, M. (2011) N-acetylglucosamine inhibits T-helper 1 (Th1)/T-helper 17 (Th17) cell responses and treats experimental autoimmune encephalomyelitis. *J. Biol. Chem.*, 286, 40133–40141.
29. Salvatore, S., Heuschkel, R., Tomlin, S., Davies, S.E., Edwards, S., Walker-Smith, J.A., French, I. and Murch, S.H. (2000) A pilot study of N-acetyl glucosamine, a nutritional substrate for glycosaminoglycan synthesis, in paediatric chronic inflammatory bowel disease. *Aliment. Pharmacol. Ther.*, 14, 1567–1579.
30. D’Haens, G., Sandborn, W.J., Feagan, B.G., Geboes, K., Hanauer, S.B., Irvine, E.J., Lemann, M., Marteau, P., Rutgeerts, P., Scholmerich, J. et al. (2007) A review of activity indices and efficacy end points for clinical trials of medical therapy in adults with ulcerative colitis. *Gastroenterology*, 132, 763–786.
31. Schroeder, K.W., Tremaine, W.J. and Ilstrup, D.M. (1987) Coated oral 5-aminosalicylic acid therapy for mildly to moderately active ulcerative colitis. A randomized study. *N. Engl. J. Med.*, 317, 1625–1629.
32. Sheridan, B.S. and Lefrancois, L. (2012) Isolation of mouse lymphocytes from small intestine tissues. *Curr. Protoc. Immunol.*, Chapter 3, Unit3 19.
33. Livak, K.J. and Schmittgen, T.D. (2001) Analysis of relative gene expression data using real-time quantitative PCR and the 2(-Delta Delta C(T)) Method. *Methods*, 25, 402–408.

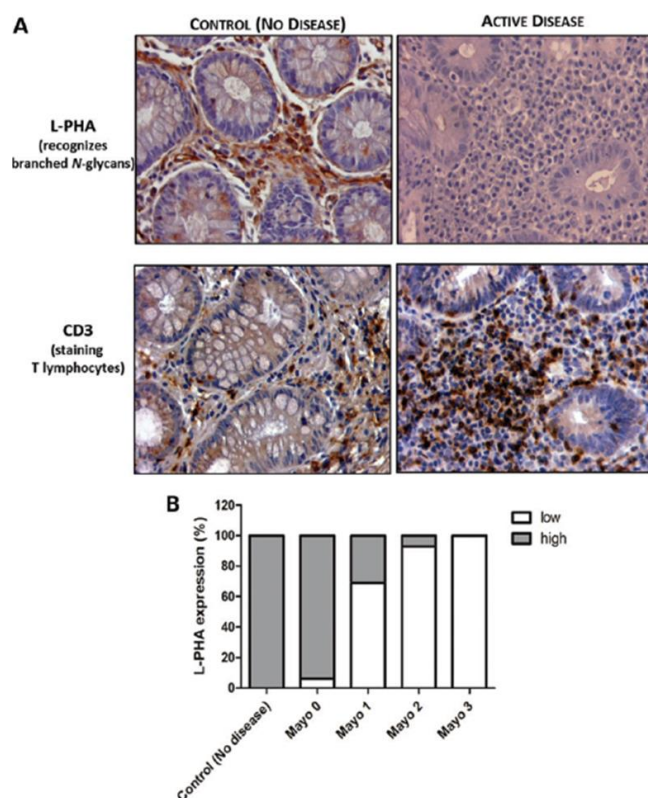


Figure 1. Relationship between the levels of lymphocytic branched N-glycans expression and the inflammatory activity. (A) A total number of 64 colonic biopsies were analyzed for L-PHA expression in the intestinal lamina propria lymphocytic infiltrate positive to CD3 expression (B). There was a significant association ( $P = 0.0001$ ) (Table 1) between the levels of lymphocytic branched N-glycans and the inflammatory activity. UC cases with active disease (Mayo subscore 1,2,3) exhibit significantly lower levels ( $\leq 25\%$ ) of L-PHA lymphocytic expression compared with normal controls. (A) Illustrates that normal controls showed a significant increased reactivity of L-PHA (.75%) in intestinal lymphocytic infiltrates CD3+ (left figures). On the contrary, right figures represent a case of active UC (Mayo subscore 3) showing a significant decrease of L-PHA reactivity in the lamina propria T lymphocytes (.25%) displaying heavy CD3 cell infiltrates. Amplification  $\times 400$ . (The evaluation of the relationship between the expression of lymphocytic b1,6 GlcNAc branched structures and the inflammatory activity considering the four percentual categories (.25%; 25–50%; 50–75% and .75%) is statistically significant (CI:95%) and the table is provided in Supplementary Material, Table S1. The regrouping in two categories (Low and High) did not change the P value and did not influence statistically the results.)

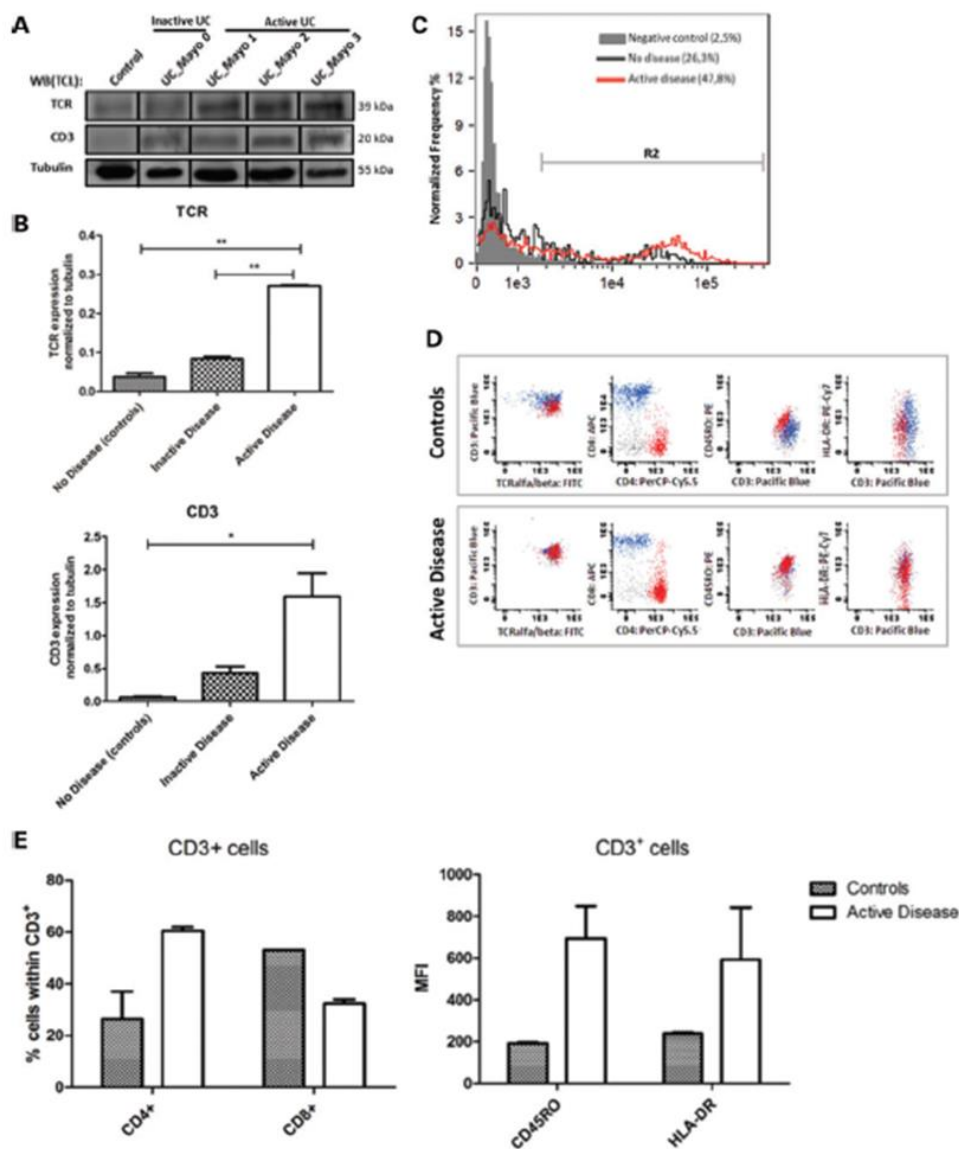


Figure 2. TCR and CD3 expression levels. (A) The results showed that active UC patients had significantly higher levels of both TCRb and CD3 expression compared with normal controls. UC patients with severe disease (Mayo subscore 3) showed the highest levels of TCRb and CD3 protein expression. Inactive UC patients (Mayo endoscopic subscore 0) exhibited an increased TCRb and CD3 expression levels compared with normal controls. (B) Bar graphs, quantification of TCRb and CD3 densities normalized to tubulin. Results are described as mean  $\pm$  SEM of three independent experiments (Student's t-test: \*  $P \leq 0.05$ ; \*\*  $P \leq 0.01$ ). In order to confirm the differential expression levels of TCRb between normal controls and active UC patients, LPLs obtained from the fresh colonic biopsies were analyzed for this marker by imaging flow cytometry (C). The percentage of cells expressing TCRb in gate R2 is indicated in brackets. The results showed that isolated LPLs from active UC patients express higher TCRb expression levels compared with normal controls. Negative control refers to unstained cells (C). Lanes in (A) were on the different gels (black lines). Characterization of the T cells subsets and activation state. (D) Flow cytometry dot-plots illustrating the CD4<sup>+</sup> (red) and CD8<sup>+</sup> (blue) T cells populations and expression of CD45RO and HLA-DR on intestinal T cells from normal individuals ( $n = 4 \pm 2$  biological replicates) and UC patients ( $n = 4 \pm 2$  biological replicates). (E) Bar graphs, showing that CD3<sup>+</sup> T cells are predominantly represented by CD4<sup>+</sup> cells in UC patients and by CD8<sup>+</sup> cells in normal individuals (left graph). The activation state of CD3<sup>+</sup> T cells was evaluated by the MFI due to antigen staining of the activation-related markers, HLA-DR and CD45RO. Intestinal T cells from UC patients exhibit a higher level of expression of these activation-related markers (right graph).

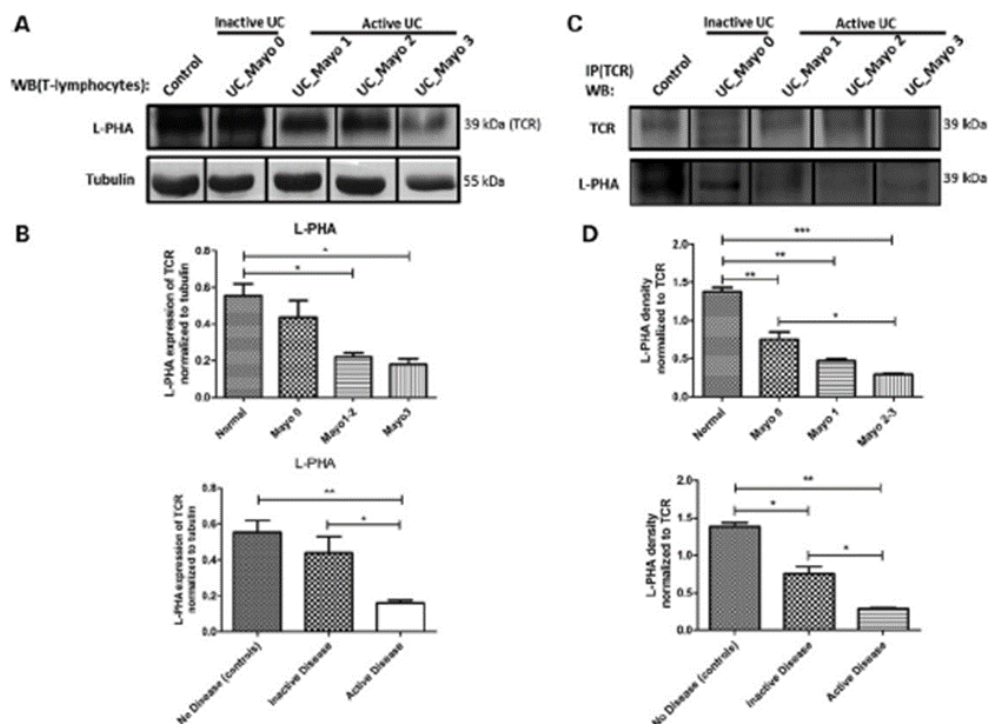


Figure 3. Alteration of intestinal TCR N-glycosylation in UC patients. (A) Protein lysates from the isolated LPLs were subjected to L-PHA lectin blot in order to evaluate the expression levels of b<sub>1</sub>,6 GlcNAc branched N-glycans on the TCR (39 kDa). The results showed a decreased TCR branched glycosylation in UC patients compared with normal controls. Patients with severe disease (Mayo subscore 3) had the lowest branched N-glycosylation modification of TCR. (B) Bar graphs, quantification of L-PHA densities on TCR band normalized to tubulin. Results are described as mean+SEM of three independent experiments (Student's t-test: \*P ≤ 0.05; \*\*P ≤ 0.01). (C) Immunoprecipitation of TCR followed by b<sub>1</sub>,6 GlcNAc branched N-glycans recognition. As observed in (A) and (B), the intestinal TCR from UC patients (with inactive and active disease) suffered a decreased modification with branched N-glycans compared with normal controls. UC patients with severe disease (Mayo subscore 3) showed the lowest levels of TCR branched N-glycosylation. (D) Bar graphs, amounts of branched N-glycan structures were determined from the ratios of densities of L-PHA reactivity normalized to TCR. Results are described as mean+SEM of three independent experiments (Student's t-test: \* P ≤ 0.05; \*\* P ≤ 0.01; \*\*\* P ≤ 0.005). Lanes in (A) and (C) were on the different gels (black lines).

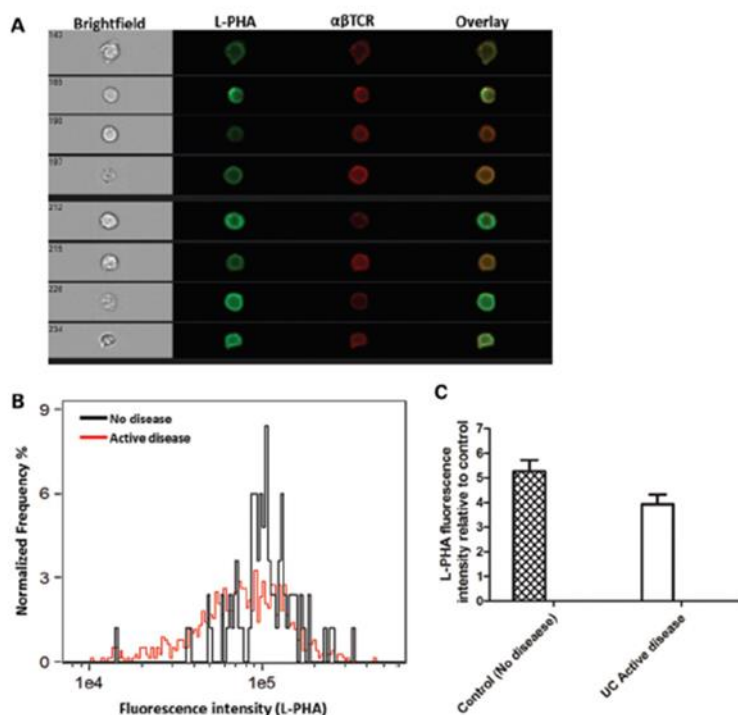


Figure 4. Imaging flow cytometry analysis of L-PHA membrane distribution in TCR positive cells. Intestinal LPLs were surface stained for TCRab and branched N-glycans (L-PHA) and analyzed on an ImageStreamX. (A) Examples of brightfield, L-PHA (green), TCRab (red) and overlaid images showing co-localization between TCRab and L-PHA. (B) Histogram representing the intensity of L-PHA staining on the TCRab+ cells. (C) The intensity of L-PHA staining on the cell membrane of TCRab+ cells was measured by imaging flow cytometry, and normalized relatively to cells stained only with streptavidin-FITC (negative control). Data show the average of two independent experiments. Error bars represent the mean+SEM. The results indicate that UC patients with active disease (Mayo subscore  $\geq 1$ ) exhibit decreased levels of L-PHA staining at the cell membrane of TCRab+ cells comparing with normal controls.

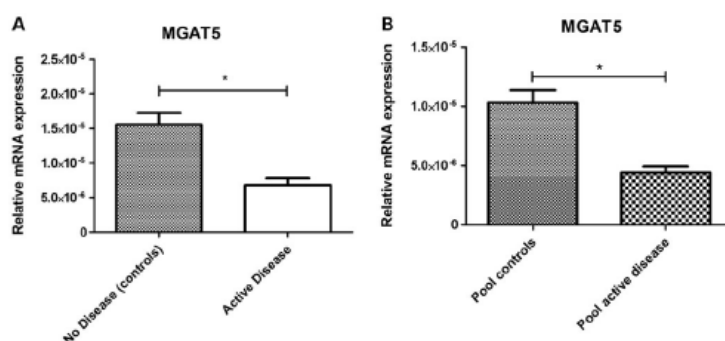


Figure 5. Deficiency of MGAT5 gene expression in LPLs from UC patients. (A) qRT-PCR analysis for mRNA expression of MGAT5 from intestinal LPLs from normal controls and active UC patients (Mayo subscore 1,2,3). Results in (A) are an average of three independent experiments, performed in triplicate, using RNA from three independent normal controls and three independent active UC patients. (B) Represents the average of two independent experiments using RNA of intestinal LPLs pooled from four different normal controls and four different UC patients, performed in triplicate. There is a significant decrease of MGAT5 mRNA expression from intestinal LPLs of UC patients (with active disease) compared with normal controls. The mRNA expression levels are expressed as mean  $\pm$  SEM (Student's t-test: \*  $P \leq 0.01$ ).

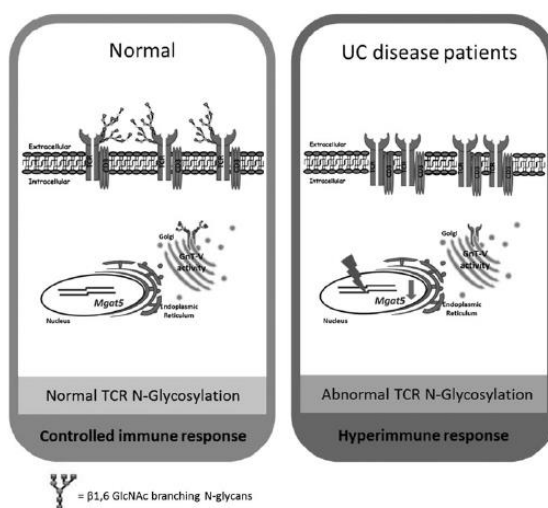


Figure 6.A model for the dysregulation of TCR N-glycosylation in UC. In intestinal homeostasis and under normal conditions, the T cell activation (TCR signaling) induces up-regulation of MGAT5 gene which in turns leads to GnT-V-mediated glycosylation of the TCR. The increased  $\beta$ 1,6GlcNAc branching synthesis on TCR, catalyzed by GnT-V, negatively regulates T cell response promoting growth arrest of T cells by raising T cell activation thresholds via limiting TCR clustering at the immunesynapse. ThisGnT-V-mediated branched glycosylation of theTCR is associated with a controlledimmune response. InUCpatients,wepropose the existence of a dysregulation of the intestinal TCR N-glycosylation catalyzed by GnT-V. Alterations on the transcription levels of MGAT5 glycogene of the intestinal T cells appear to underlie the deficiency of GnT-V-mediated glycosylation on the TCR. This dysregulation of TCR branched N-glycosylation contribute to decrease the threshold of T-cell activation leading to a hyperimmune response, which is a feature of UC patients.

L-PHA expression (%) in intestinal lymphocytic infiltrate				<i>P</i> -value
Clinical features	Number of cases ( <i>n</i> = 64)	Low	High	
Inflammatory activity				<0.0001
Control (no disease)	13	0	13 (100%)	
Inactive disease (Mayo 0)	16	1 (6.25%)	15 (93.75%)	
Active				
Mayo 1	13	9 (69.23%)	4 (30.77%)	
Mayo 2	14	13 (92.86%)	1 (7.14%)	
Mayo 3	8	8 (100%)	0	

Table 1. Relationship between L-PHA expression in intestinal lymphocytic infiltrate and the inflammatory activity

	Patients' characteristics	
	Controls	UC patients
<i>n</i>	13	17
Gender (M/F)	7/6	8/9
Age, range (years)	30–89	25–62
Age, mean (years)	68	45

Table 2. Patients' characteristics